NUMERICAL FEL STUDIES WITH A NEW CODE ALICE

Igor Zagorodnov and Martin Dohlus
DESY, Hamburg, Germany

Abstract

We present a fully three dimensional time-domain simulation code for free-electron lasers. Compared to the existing codes, we have implemented different numerical schemes for tracking and field calculations. The equations of motion of the particles are integrated with a "leap-frog" scheme. The parabolic field equation is resolved with implicit Neumann finite difference scheme based on azimuthal expansion. Additionally, we have implemented the open boundary condition with the help of perfectly matched layer for parabolic equation. The last feature allows for a mesh only in the bunch vicinity. The implemented field solver is accurate and fast. We prove the accuracy of the code with different numerical tests and apply the code to estimate the expected properties of the radiation in FLASH facility with 3rd harmonic module.

INTRODUCTION

An accurate self consistent simulation of collective effects in the charged beams remains a challenging problem for numerical analysis. During the last decades several numerical codes are developed to model the non-linear process in a self-amplified spontaneous emission (SASE) free electron lasers (FEL). In this paper we present a new numerical code which is based on the mathematical model used earlier in such three dimensional (3D) codes as TDA [1], FAST [2], Genesis 1.3 [3], GINGER [4]. However, we have implemented different numerical schemes for tracking and field calculations. The equations of motion of the particles are integrated with symplectic "leap-frog" scheme. The parabolic field equation is resolved with implicit Neumann finite difference scheme based on azimuthal expansion. Additionally we have implemented the open boundary condition with the help of perfectly matched layer (PML) for parabolic equation. The last feature allows for a mesh only in the bunch vicinity. The implemented field solver is accurate and fast. The code is parallelized and allows to use one dimensional, rotationally symmetric or fully three dimensional models. We prove the accuracy of the code with different numerical tests and apply the code to estimate the expected properties of the radiation in FLASH facility with 3rd harmonic module.

FEL CODE DESCRIPTION

Mathematical Model

Following the approach of [1] the equations of motion for helical undulator can be derived from Hamiltonian

$$h(\vec{r}_\perp, ct; \vec{P}_\perp, P_t; z) = -\gamma\left[1-\gamma^{-2}\left(1+\left|\vec{P}_\perp\right|^2+\left|\vec{a}_\perp\right|^2\right)\right]^{0.5} + a_z .$$

The squared module of the transverse part of the vector potential $\vec{a} = e\vec{A}/(mc)$ can be approximated as

$$\left|\vec{a}_\perp\right|^2 = K^2 + 2a_s K \sin(\psi + \varphi_s) .$$

Here $\psi = (k + k_w)z - \omega t$ is a particle phase, K is an averaged undulator parameter, $a_s \exp(i\varphi_s)$ is a normalized complex amplitude of the amplified wave

$$A_x^s + iA_y^s = -imce^{-1}a_s e^{i(kz-\omega t+\varphi_s)}, \quad E^s = -\frac{\partial}{\partial t}A^s .$$

The canonical moments are defined by relations

$$\vec{P}_\perp = \gamma\frac{d\vec{r}_\perp}{dz}\beta_z - \vec{a}_\perp, \quad P_t = -\gamma + \frac{e}{mc^2}\varphi .$$

The equations of motion read

$$\frac{d\psi}{dz} = k_w - k(2\gamma^2)^{-1}\left(1+\left|\vec{P}_\perp\right|^2 + K^2\right),$$

$$\frac{d\gamma}{dz} = \frac{k}{\gamma\beta_z}Ka_s\cos(\psi+\varphi_s) - \frac{e}{mc^2}E_z, \quad \frac{d\vec{r}_\perp}{dz} = \frac{\vec{P}_\perp}{\gamma\beta_z},$$

$$\frac{dP_x}{dz} = -\left(\frac{K^2k_x^2}{\gamma\beta_z}+\frac{eg}{mc}\right)x, \quad \frac{dP_y}{dz} = -\left(\frac{K^2k_y^2}{\gamma\beta_z}-\frac{eg}{mc}\right)y .$$

We split the electromagnetic field in the transverse and longitudinal components. The longitudinal electrostatic field results from the bunching and can be suggested to be a nearly periodic one. Then the Fourier components of the longitudinal field can be found from the equation [1]

$$\left(\nabla_\perp^2 - \frac{n^2(k+k_w)^2}{\gamma_z^2}\right)E_z^{(n)} = \frac{in(k+k_w)}{\varepsilon_0\gamma_z^2}\rho^{(n)},$$

$$\rho^{(n)}(\vec{r}_\perp) = \frac{1}{2\pi}\int_0^{2\pi}\rho(\vec{r}_\perp,\psi)e^{-in\psi}d\psi = -\frac{I}{Nv_z}\sum_{i=1}^{N}e^{-in\psi_i}\delta(\vec{r}_\perp - \vec{r}_{i\perp}) .$$

The transverse field components fulfil the parabolic equation

$$\left[\nabla_\perp^2 + 2ik\frac{d}{dz}\right]E^s = i\theta_s\omega\frac{v_z\rho^{(1)}}{c^2\varepsilon_0} .$$

If the Pierce parameter $\rho = c\gamma_z^{\,2}\Gamma\omega^{-1}$ is small and the transverse variation of the longitudinal field can be neglected than the following set of normalized [5] equations can be considered

$$\hat{x}'' = -\left(\hat{k}_x^{\,2} + \hat{g}\right)\hat{x}, \quad \hat{y}'' = -\left(\hat{k}_y^{\,2} - \hat{g}\right)\hat{y}, \qquad (1)$$

$$\frac{d\psi}{d\hat{z}} = \hat{C} + \hat{P} - \frac{B}{2}(\hat{x}'^2 + \hat{y}'^2), \quad \frac{d\hat{P}}{d\hat{z}} = \left|\hat{u}\right|\cos(\psi+\psi_r) - \hat{E}_z,$$

$$\hat{E}_z = \hat{E}_z^{(0)} - \hat{\Lambda}_p^{\,2}\frac{1}{N_{jk}}\sum_{i=1}^{N_{jk}}\left[\pi\,\mathrm{sgn}(\psi-\psi_i) - (\psi-\psi_i)\right],$$

$$\left[\frac{1}{2iB}\hat{\Delta}_\perp + \frac{d}{d\hat{z}}\right]\hat{u}\left(\vec{\hat{r}}_\perp, \hat{z}, \frac{\hat{z}-\hat{z}_0}{c}\right) = -2a^{(1)}\left(\vec{\hat{r}}_\perp, \hat{z}, \frac{\hat{z}-\hat{z}_0}{c}\right),$$

where $\hat{x} = xr_0^{-1}$, $\hat{y} = yr_0^{-1}$, ($r_0 = \sqrt{2\sigma_x\sigma_y}$) are transverse particle coordinates, $\hat{P} = (\gamma - \gamma_0)(\gamma_0\rho)^{-1}$ is an energy deviation, $\hat{C}$ is a detuning parameter, $\hat{u}$ is the transverse (in complex notation) electric field and $\hat{E}_z$ is the longitudinal electric field. The other parameters in Eq. (1) are defined as in [5] with 1D normalization of Chapter 1.

Numerical Scheme

At the beginning we divide the bunch longitudinally in N_s slices (numerated from the tail) with the length equal to the radiation wavelength. The initial particle distribution in the slice is generated with the "quiet start" method [6]. For this purpose we use the Sobol sequences [11] and the inverse error function. The noise statistics in the slice is imposed as described in [7]. The transverse mesh is constructed in polar coordinates with N_r divisions along the radius and N_φ divisions along the angle. Each slice is tracked through the undulator with N_z periods. The elementary volume V_{pqt}, $p = 1:N_s$, $q = 1:N_r$, $t = 1:N_\varphi$, contains N_{pqt} macroparticles [7].

The discrete equations of motion are

$$\frac{\psi_{i,j+0.5} - \psi_{i,j-0.5}}{\Delta\hat{z}} = \hat{P}_{ij} + \hat{C}_j - \frac{B}{2}\left(\hat{x}'^2_{ij} + \hat{y}'^2_{ij}\right),$$

$$\frac{\hat{P}_{i,j+1} - \hat{P}_{i,j}}{\Delta z} = \frac{\hat{u}^{p,q,t}_{j+1} + \hat{u}^{p,q,t}_{j}}{2} + \left[\psi_{i,j+0.5} + \frac{\theta^{p,q,t}_{j+1} + \theta^{p,q,t}_{j}}{2}\right] + \hat{E}^{p,q,t}_{z,j+0.5},$$

$$\begin{pmatrix}\hat{x}_{i,j+1}\\ \hat{x}'_{i,j+1}\end{pmatrix} = M_x\begin{pmatrix}\hat{x}_{i,j}\\ \hat{x}'_{i,j}\end{pmatrix}, \qquad \begin{pmatrix}\hat{y}_{i,j+1}\\ \hat{y}'_{i,j+1}\end{pmatrix} = M_y\begin{pmatrix}\hat{y}_{i,j}\\ \hat{y}'_{i,j}\end{pmatrix},$$

$i = 1:N_p$, $j = 1:N_z$.

To find the transverse field we use the Fourier transform in azimuthal coordinate. For each azimuthal mode m we have to solve the parabolic equation (in a simplified notation)

$$\left[\frac{1}{2iB}\frac{1}{r}\frac{\partial}{\partial r}r\frac{\partial}{\partial r} - \frac{m^2}{r^2} + \frac{d}{dz}\right]u^{(m)} = -2a^{(1)(m)}, r \in (0,\infty), \quad (2)$$

with the condition on the axis

$$\frac{\partial}{\partial r}u^{(0)}(0) = 0,\ u^{(m)}(0) = 0,\ m > 0.$$

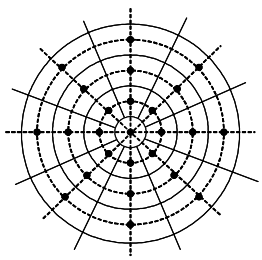

Figure 1: The transverse mesh.

In order to truncate the mesh at radius r_0 we use an absorbing layer called perfectly matched layer [8], which possesses the desired property of generating very low numerical reflection. In order to construct a mathematical model of the PML we introduce the complex variable

$$\tilde{r} = r + \frac{i}{B}\int_0^r \sigma(\xi)d\xi, \qquad \sigma(r) = \begin{cases}0, & r \le r_0\\ \ge 0, & r > r_0\end{cases}.$$

The change of the variable r to $\tilde{r}$ (and the partial derivative $\partial/\partial r$ to $\partial/\partial\tilde{r}$) in Eq. (2) will give us the required equation. This change of variable does not alter the solution in the area of interest ($r < r_0$), but it extends the solution by a fast exponentially decaying part in the absorbing layer $r_0 < r < r_{PML}$.

Let us introduce the radial mesh

$$\tilde{r}_j = \tilde{r}_{j-1} + \frac{i}{B}\sigma_{j-0.5}\Delta r, \quad j = 1:n_r,\ n_r = r_0/\Delta r,$$

$$\sigma_{j-0.5} = \begin{cases}0, & j \le n_r,\\ B\dfrac{10}{\Delta r}\left(\dfrac{r_{j-0.5}}{L_{PML}}\right)^2,\end{cases}$$

$$r_{j-0.5} = (j - n_r - 0.5)\Delta r, \quad L_{PML} = r_{PML} - r_0.$$

The implicit Neumann numerical scheme reads

$$c_q u^{n+1}_{q+1} + b_q u^{n+1}_q + a_q u^{n+1}_{q-1} = f^n_q,$$

$$c_q = \frac{\Delta z}{4iB}\frac{1}{\tilde{r}_j}\frac{\tilde{r}_{j+0.5}}{(\tilde{r}_{j+0.5} - \tilde{r}_{j-0.5})(\tilde{r}_{j+1} - \tilde{r}_j)},$$

$$a_q = \frac{\Delta z}{4iB}\frac{1}{\tilde{r}_j}\frac{\tilde{r}_{j-0.5}}{(\tilde{r}_{j+0.5} - \tilde{r}_{j-0.5})(\tilde{r}_j - \tilde{r}_{j-1})},$$

$$b_q = (1 - a_q - c_q) - \frac{\Delta z}{iB}\frac{m^2}{\tilde{r}_j^2},$$

$$f^n_q = -c_q u^n_{q+1} + (2 - b_q)u^n_q - a_q u^n_{q-1} - 2\Delta z_f a^{(1)}(q).$$

We supply this scheme with the discrete boundary condition at r_{PML}

$$a_{n_r+n_{PML}} = c_{n_r+n_{PML}} = f^n_{n_r+n_{PML}} = 0;\ b_{n_r+n_{PML}} = 1; \qquad m \ge 0,$$

and a discrete boundary condition at $r = 0$. The last condition for the monopole mode reduces to

$$c_0 = \frac{\Delta z}{iB}\frac{1}{\Delta r^2},\ a_0 = 0,\ b_0 = 1 - c_0,$$

$$f^n_0 = -c_0 u^n_1 + (2 - b_0)u^n_0 - 2\Delta z a^{(1)}(0),$$

and for higher order modes it reads

$$a_0 = c_0 = f^n_0 = 0;\ b_0 = 1; \quad m > 0.$$

Figure 1 sketches the used transverse mesh. The black points present the location of sample points for the field.

NUMERICAL RESULTS

Numerical Tests

Figure 2 shows a simulation of the propagation of the fundamental Gaussian mode in free space. To truncate the mesh we use different boundary conditions. The Dirichlet

boundary condition, $\hat{u}(\hat{r}_0)=0$, spoils the solution very fast. The absorbing PML produces the accurate results.

In FEL simulations the Dirichlet boundary condition works satisfactory in the exponential growth regime (linear regime), but it could spoil the correct solution after the saturation (non-linear regime). Figure 3 shows a 3D simulation for a round beam with radius $\hat{r}_b=1$. It can be seen that for the Direchlet condition the mesh should be truncated very far from the beam (at $\hat{r}_0=10$). On the contrary, the quite thin perfectly matched layer (only 7 mesh points) allows to truncate the mesh accurately already at radius $\hat{r}_0=2$.

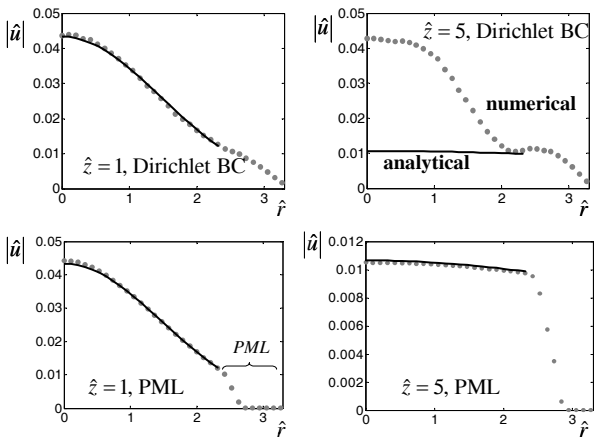

Figure 2: Propagation of the Gaussian mode with PML.

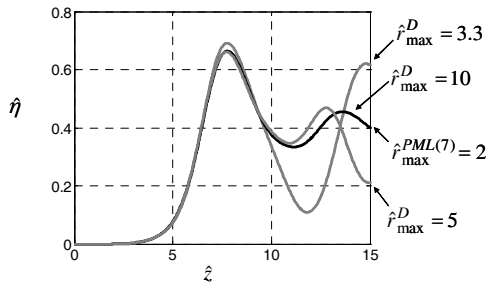

Figure 3: The radiation power with and without PML.

Figure 4 presents a comparison with the code Genesis 1.3 [3]. We carry out a simulation with only one slice in amplifier model. The space of parameters corresponds to SASE2 undulator at wavelength of 0.1 nm as described in [9]. The left plot compares the radiation power at saturation. The first comparison was done in the January 2008 [10] (version 1.0 of Genesis 1.3). The disagreement in the saturation power at the level of 20 % was obtained. After thorough analysis we have found that the particle distribution generated in Genesis 1.3 had a wrong statistics as can be seen from the right plot, where the error in the fourth moment is shown. The used in Genesis 1.3 the "Box-Mueller" algorithm [11] (to convert the uniform distribution to Gaussian one) has spoiled the "quiet-start" property and the statistics of the particle distribution. Our code ALICE uses an inverse error function to implement such conversion. It conserves "quiet-start" property of the initial distribution. The new version 2.0 of Genesis 1.3 released in April 2008 allows to use the inverse error function transformation (parameter inverfc=1). With this option results obtained by the both codes converge together.

Figure 5 shows a comparison of the results obtained in the time-dependent model for SASE case. In the left plot the grey curve presents the radiation energy in the pulse as obtained with code Genesis 1.3. The black line shows the result from the code ALICE and the both curves coincide. The simulations have been done with 60000 particles in the slice. The right plot presents the radiation power along the bunch averaged longitudinally through 1500 slices. Again we see good agreement in the temporal structure of the radiation.

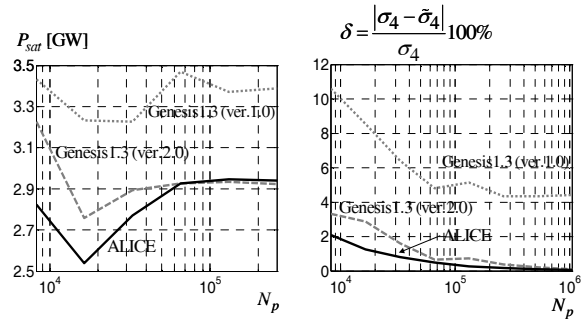

Figure 4: Comparison with Genesis. Periodic model.

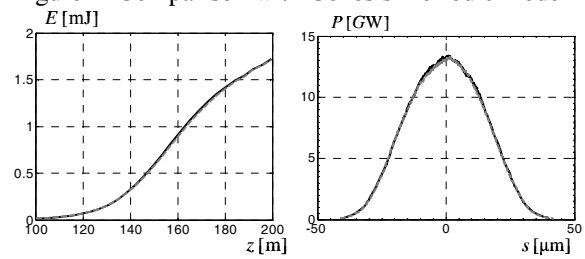

Figure 5: Comparison with Genesis. SASE model.

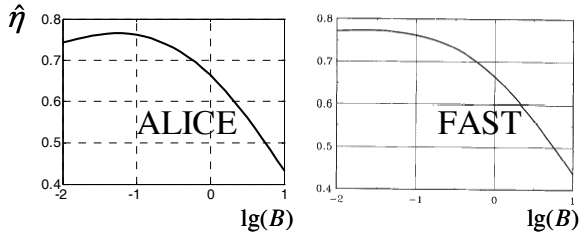

Figure 6: Comparison with FAST. Periodic model.

In order to test the code we have reproduced with it most of the numerical results obtained with code FAST [2] and published in [5]. For example, Figure 6 shows the reduced efficiency at saturation versus the diffraction parameter B.

Expected Radiation in the FLASH with 3rd Harmonic Module

In order to linearize the energy chirp before the first bunch compressor the third harmonic module will be installed at FLASH at the end of 2009.

To find working points, to define the tolerances and to characterize the parameters of the bunch at the undulator entrance we have done series of "start-to-undulator" simulations for different bunch charges [12].

In these simulations we have tried to take into account the most important "self-fields" such as wake fields, space-charge fields and synchrotron radiation in the bunch compressors. The tracking was done with a simple one dimensional model like that used in Litrack code of K. Bane [13]. The results were checked with full 3D simulations with codes ASTRA [14], CsrTrack [15] and GlueTrack [12].

Figure 7 shows the longitudinal phase space as obtained by 1D and 3D tracking. The right plot presents the charge density in the longitudinal phase space.

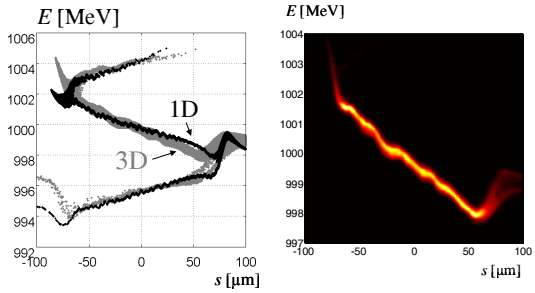

Figure 7: Longitudinal phase space for 1 nC.

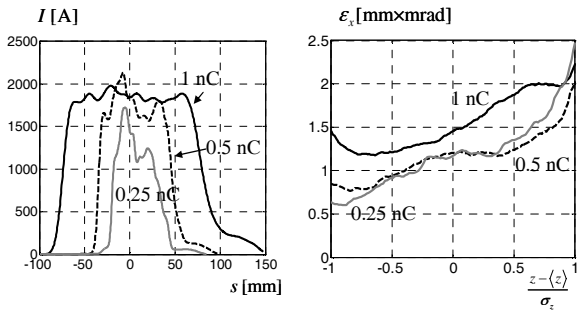

Figure 8: Current and emittance for different charges.

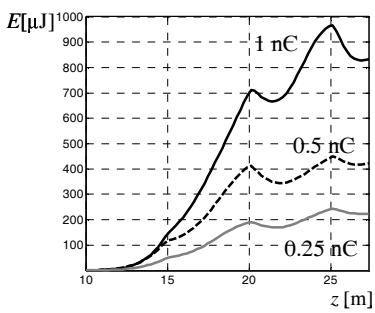

Figure 9: Radiation energy.

The left plot in Figure 8 describes the current profiles at the undulator entrance for bunches with different charges. The right figure shows the horizontal emittance in the bunch core. The bunch compressors in FLASH are oriented horizontally and have negligible impact on the vertical emittance, which is in our simulations always smaller then the horizontal one.

We have extracted the all slice parameters from the particle distributions and used them to carry out full three dimensional FEL simulations with code ALICE.

Figure 9 presents the evolution along the undulator of the radiation energy in SASE mode for different bunch charges. The full set of plots for different characteristics of the obtained radiation can be found in [16].

Table 1: Radiation Properties

	With 3rd harmonic module			Without [17]
Charge, nC	1	0.5	0.25	0.5-1
Wavelength, nm	6.5	6.5	6.5	6
Bunch energy, MeV	1000	1000	1000	1000
Peak current, kA	2	2	1.7	1.3-2.2
Slice emittance, mkm	1.2-2	0.7-2	0.6-2	1.5-3.5
Saturation length, m	20	20	20	22-32
Energy in the radiation pulse, mkJ	700	400	200	50-150
Radiation pulse duration at 80% of contrast, fs	200-300	100-200	50-140	
Radiation pulse duration FWHM, fs	100-250	35-150	25-100	15-50
Averaged peak power, GW	3	3	3	2-4
Spectrum width, %	0.4-0.5	0.4-0.5	0.4-0.5	0.4-0.6
Coherence time, fs	4-5	4-5	4-5	

The main characteristics of the radiation are collected in Table 1. The right column gives for comparison the results obtained in [17] for the scenario without the third harmonic module.

REFERENCES

[1] T.M. Tran, J.S.Wurtele, Phys. Reports 195 (1990) 1
[2] E.L.Saldin et al, NIM A 429 (1999) 233.
[3] S. Reiche, NIM A 429 (1999) 243.
[4] W.M. Fawley, LBNL CBP Tech Note-104 (1995).
[5] E.L. Saldin et al, The Physics of Free Electron Lasers, Springer (1999).
[6] J.M.Dawson, Rev. of Modern Physics 55 (1983) 403
[7] W.M. Fawley, Phys. Rev. STAB 5 (2002) 070701.
[8] F. Collino, J. Comp. Phys. 131 (1997) 164
[9] The European X-Ray Free Electron Laser TDR, DESY 2006-097 (2006).
[10] I.Zagorodnov, Genesis/ALICE benchmarking (2008), http://www.desy.de/xfel-beam/talks_a.html#
[11] W.H.Press et al, Numerical Recipes in C, Cambridge University Press (1988).
[12] I.Zagorodnov, Beam dynamics in FLASH with 3rd harmonic module (2009) (see ref. [10]).
[13] K.L.F Bane and P.Emma, SLAC-PUB-11035 (2005).
[14] K. Flöttmann, ASTRA User manual (2000), http://www.desy.de/~mpyflo/
[15] M. Dohlus, TESLA-FEL-2003-05, DESY, 2003.
[16] I.Zagorodnov, Expected radiation in FLASH with 3rd harmonic module (2009) (see ref. [10]).
[17] E.L.Saldin at al, TESLA FEL 2004-06 (2004).